

Reactor scale up for biological conversion of cellulosic biomass to ethanol

Xiongjun Shao · Lee Lynd · André Bakker ·
Richard LaRoche · Charles Wyman

Received: 8 May 2009 / Accepted: 16 July 2009 / Published online: 2 August 2009
© Springer-Verlag 2009

Abstract The absence of a systematic scale-up approach for biological conversion of cellulosic biomass to commodity products is a significant bottleneck to realizing the potential benefits offered by such conversion. Motivated by this, we undertook to develop a scale-up approach for conversion of waste paper sludge to ethanol. Physical properties of the system were measured and correlations were developed for their dependence upon cellulose conversion. Just-suspension of solid particles was identified as the scale up criterion based on experiments at lab scale. The impeller speed for just solids suspension at large scale was predicted using computational fluid dynamics simulations. The scale-up strategy was validated by analyzing mixing requirements such as solid–liquid mass transfer under the predicted level of agitation at large scale. The scale-up approach enhances the prediction of reactor performance and helps provide guidelines for the analysis and design of large scale bioreactors based on bench scale experimentation.

Keywords CFD · SSF · Scale up · Solids suspension · Cellulosic biomass

List of symbols

$[C]$	Cellulose concentration (g/L)
$[Cb^*]$	Cellobiose concentration in interface (g/L)
$[Cb]$	Cellobiose concentration (g/L)
$[CE]$	Cellulose–enzyme complex concentration (g/L)
$[I]$	Solids concentration (g/L)
$[X]$	Xylan concentration (g/L)
a_p	Particle surface area per volume (m^{-1})
C_{pL}	Liquid heat capacity [J/(kg K)]
D	Impeller diameter (m)
Da_M	Damkoehler number
ΔT	Temperature difference between tank inner surface and bulk liquid ($^{\circ}C$)
d_p	Particle diameter (m)
ε	Power per mass on liquid or turbulent kinetic energy dissipation rate (W/kg)
Eth	Ethanol
ϕ	Solids loading (g/L)
h_i	Heat transfer coefficient in inner tank surface [W/($m^2 K$)]
k	Thermal conductivity [W/(m K)]
$k(x)$	Conversion dependent rate constant of cellulose hydrolysis (h^{-1})
k_r	Reaction constant (s^{-1})
k_t	Turbulent kinetic energy (m^2s^{-2})
k_{SL}	Solid–liquid mass transfer coefficient (m/s)
M_k	Mass transfer rate (g/(L s))
M_r	Reaction rate, g/(L s)
μ_L	Liquid viscosity (cp)
N	Operating impeller speed (s^{-1})
N_{js}	Just-suspended speed at large scale (rpm)

X. Shao · L. Lynd (✉)
Thayer School of Engineering at Dartmouth College,
Hanover, NH 03755, USA
e-mail: lee.lynd@dartmouth.edu

X. Shao
e-mail: xiongjun.shao@dartmouth.edu

A. Bakker
ANSYS, Inc., Lebanon, NH 03766, USA

R. LaRoche
DEM Solutions, Lebanon, NH 03766, USA

C. Wyman
Chemical and Environmental Engineering,
University of California Riverside,
Riverside, CA 92521, USA

N_{js0}	Just-suspended speed at small scale (rpm)
P	Power (W)
P_{js}	Power for just solids suspension (W)
ρ_{ave}	Average density for reactor content (g/L)
ρ_{H_2O}	Water density (g/L)
ρ_L	Liquid density (g/L)
P_o	Power number of impeller, 1.5 for the marine impeller
Pr	Prandtl number
ρ_S	Solids density (g/L)
Q	Total heat of production by reaction (J)
r	Rate of reaction or heat production (g/(L s)) or (J/g)
Re	Reynolds number
S	Tank wall surface area (m ²)
Sc	Schmidt number
Sh	Sherwood number
σ	Quality of solids suspension as defined in Eq. 3
T	Large scale tank diameter (m)
T_0	Small scale tank diameter (m)
τ_B	Mixing/blend time (s)
t_r	Characteristic reaction time (s)
V	Tank volume (m ³)
VF	Volume fraction
w_{H_2O}	Amount of water added to flask (g)
w_S	Weight of solids sample added to volumetric flask (g)
x	Conversion

Introduction

Production of biocommodity products such as fuel ethanol through biological conversion of cellulosic biomass offers benefits with respect to sustainable resource supply [1, 2], energy security, rural economic development [3, 4], and green house gas emission reduction [5–8]. The primary strategic obstacle to realizing these benefits is the high current cost of overcoming the recalcitrance of cellulosic biomass. Other important issues must also be addressed, and these include developing systematic scale-up procedures. A reliable scale up strategy could reduce risk, inform process decisions, and reduce cost from pilot and demonstration operations.

For reaction systems involving particulate reacting material, the minimum impeller speed to suspend all the particles (just-suspended speed), N_{js} is usually the optimal operating point with respect to enhancing solid–liquid mass transfer by the intensity of agitation [9]. This phenomenon was observed experimentally by Elander [10] on enzymatic

hydrolysis of Solka-floc and by Huang [11] on hydrolysis of amorphous cellulose. A common approach to scale up on the basis of N_{js} is to find the exponent, n in Eq. 1 for the rotational speed of the impeller.

$$N_{js} \sim \left(\frac{T}{T_0}\right)^{-n} N_{js0} \quad (1)$$

Constant exponents were reported by some studies [12–14], whereas variable exponents were found by Corpstein et al. [15] to be a function of particle settling velocity and by Geisler et al. [16] to find the two extremes of scaling up based on either power per mass ($n = 2/3$) or constant tip speed ($n = 1$) through some assumptions and simplified calculations. Computational fluid dynamics (CFD) is a rigorous and state-of-the-art tool that can be applied to predict N_{js} at different scales.

This study considers the issue of scaling up bioreactors featuring simultaneous saccharification and fermentation (SSF) using waste paper sludge in a cascade CSTR configuration. Lab scale experiments are performed to determine the desired degree of mixing or the scale up criterion. CFD simulations are employed to calculate the mixing power requirement at large scale. Other mixing requirements such as solid–liquid mass transfer at large scale are analyzed using a combination of industrial mixing analysis and CFD simulations.

Materials and methods

Materials

Waste paper sludge used in this study was obtained from the Fraser Mill, Gorham, NH and stored in ~1L aliquots in a large freezer at –23 °C. Composition and SSF tests for the sludge have been reported in a previous study [17]. Spezyme CP cellulase was kindly provided by Genencor International, Inc. Novozyme 188 β -glucosidase was obtained from Sigma-Aldrich (St. Louis, MO). The activities of the cellulase and the β -glucosidase were 57 FPU per mL and 1,100 IU per mL respectively determined using the protocols reported by Ghose [18]. Cellulase was supplemented by β -glucosidase with an activity ratio of 1:3 for SSF experiments. *Saccharomyces cerevisiae*, strain D5A (NREL), prepared in YPD media (Sigma Y1375) was used for SSF inoculation. The growth medium developed by Kadam and Newman [19] consisting of 0.3% (v/v) corn steep liquor supplemented by 5 mM MgSO₄ was used in all SSF experiments. The concentrations of SSF products were obtained using HPLC with an Aminex HPX-87H column at 65 °C.

Experiments for desired degree of mixing/scale-up criterion

The desired degree of mixing can be determined by examining the reactor performance (incremental conversion or ethanol concentration) at various mixing intensities. A schematic diagram of the experimental reactor system configuration is shown in Fig. 1. A 21-L glass carboy containing 18 L of paper sludge-containing growth medium with 90 g/L of cellulose was sterilized for 12 hours at 121 °C. The glass carboy was equipped with an impeller with two flat blades and a Bellco overhead motor (No. 7764-00110) rated at 115 W. Batch SSF experiments were initiated with a cellulase loading of 12 U/g cellulose. 1.6 L of the partially reacted carboy content were distributed using a MasterFlex pump (No. 7520-35) into each of the four pre-sterilized 3-L Applikon bioreactors when conversion was at 35% and 60%. Impeller speed in each bioreactor was controlled by an Applikon stirrer controller (P100-ADI 1032). The reaction was allowed to continue for 8 and 24 h respectively for the two conversions with various impeller speeds in the four bioreactors. Temperature in both the carboy and the bioreactors was kept at 37 °C with heating blankets controlled by Delta-V system via an Applikon Bio Console (ADI 1025).

Measurement of physical properties

Physical properties, required for industrial mixing analysis and CFD simulation, were measured and correlated with cellulose conversion. Batch SSF was conducted in a 3-L fermenter with a cellulose concentration of 90 g/L and a cellulase loading of 12 U/g cellulose. Duplicate samples

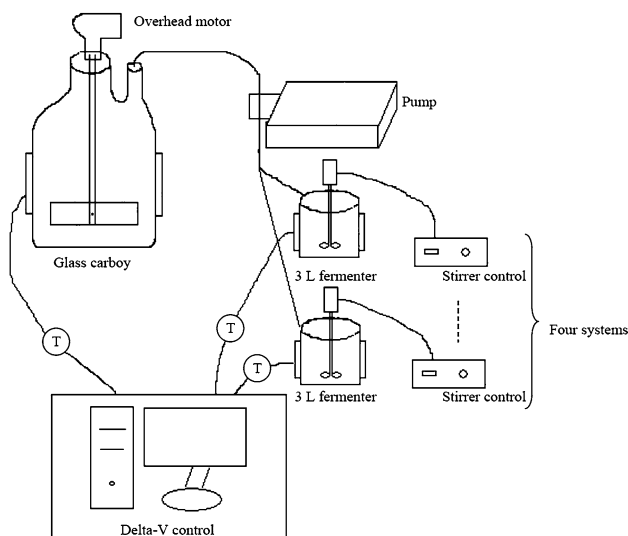


Fig. 1 Schematic diagram of the reactor system configuration for desired degree of mixing

were taken after 30.5, 51, 72, 95.5, and 143.5 h of reaction. The samples were centrifuged. Supernatant samples were taken to measure the concentrations of hydrolysis and fermentation products using HPLC, the liquid density at room temperature using a 1 mL volumetric flask, and the liquid viscosity using a Cannon Fenske certified viscometer (No. 50-541A) at 37 °C. One set of solid samples were washed twice with 30 mL DI water, re-suspended with 30 mL DI water, and sterilized at 121 °C for 30 min. The samples were then sent to Particle Technology Labs (Westmont, IL) for particle size measurement. The other set of solid samples were washed twice with 30 mL DI water and dried in a 100 °C oven (Precision Model 45 EG) for measuring solids density using a 10 mL volumetric flask and an analytical balance. The solids density was calculated using the following equation

$$\rho_s = \frac{w_s}{0.01 - \frac{w_{H_2O}}{\rho_{H_2O}}} \tag{2}$$

where w_s is the weight of solid sample added to the volumetric flask, and w_{H_2O} is the amount of water added to the flask to reach 10 mL total volume.

Reactor configurations for scale up analysis

A cascade CSTR reactor configuration was selected for the analysis. The analysis was performed in the first reactor only. The mixing requirements for subsequent reactors are less than that for the first reactor because of lower viscosity with increasing conversion. A typical conversion of 48% for the first reactor was chosen based on kinetic models described elsewhere [17, 20] for the analysis with an initial cellulose concentration of 90 g/L. The reactor geometry for the analysis was based on an Applikon 3-L bioreactor with 1.6 L working volume. The reactor was equipped with three baffles, a thermometer well, and a marine type impeller with a power number of 1.5 calculated using FLUENT. A picture of the reactor geometry is shown in Fig. 2. The dimensions for the geometry are presented in Table 1.

Fluent modeling

The reactor geometry shown in Fig. 2 was created using GAMBIT software and split into a moving zone containing the impeller and a stationary outer zone, which were meshed with 123,240 and 475,465 grid cells, respectively. The shaft, impeller, baffles, temperature tube, tank bottom, and tank walls were specified with WALL boundary conditions, while the top surface was specified with the SYMMETRY boundary condition. The mesh and boundary conditions were exported from GAMBIT and imported to FLUENT. N_{js} at lab scale was first simulated. The quality

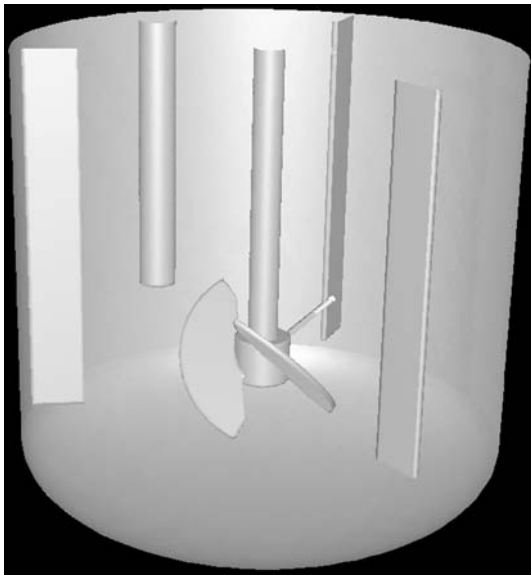


Fig. 2 Picture of reactor geometry for scale up analysis

Table 1 Dimension of the reactor geometry for scale up analysis

Parameter	Lab scale	Large scale
Tank diameter (T)	0.13 m	15.24 m
Liquid height	0.13 m	15.24 m
Impeller diameter (D)	0.0455 m	5.334 m
Baffle thickness	0.0015 m	0.176 m
Baffle width	0.014 m	1.64 m
Baffle height	0.096 m	11.25 m
Bottom clearance (C/T)	0.354	0.354
Temperature tube length	0.077 m	9.03 m
Temperature tube OD	0.0105 m	1.23 m
Baffle spacing	120°	120°
Baffle clearance	0.003 m	0.352 m
Temperature tube position	$r = 0.051$ m, 60° from baffle	$r = 5.98$ m, 60° from baffle

of solids suspension, σ , corresponding to the volume weighted average (A) of relative difference between the average solids volume fraction and the local solids volume fraction, was calculated using Eq. 3. N_{js} at large scale was predicted by achieving the same level of σ as lab scale.

$$\sigma = A \left\{ \text{abs} \left(\frac{VF_{\text{ave}} - VF_{\text{local}}}{VF_{\text{ave}}} \right) \right\} \quad (3)$$

Heat transfer was simulated by specifying a constant temperature on the tank wall iteratively to balance the heat produced by reaction and to keep the reactor at 37 °C. At steady state, the rate of ethanol production can be

calculated from Eq. 4. With a heat of reaction of 54 kcal per mole of glucose consumed, Eq. 5 was derived to obtain the rate of heat production.

$$r_{\text{Eth}} = \frac{1}{\tau} [\text{Eth}] \left(\frac{\text{g}}{\text{L s}} \right) \quad (4)$$

$$r_{\text{heat}} = 2.46 \times 10^6 r_{\text{Eth}} \left(\frac{\text{J}}{\text{g}} \right) \quad (5)$$

For a residence time of 1 day and a cellulose conversion of 48%, the rate of ethanol production is 0.000244 g/(L s) and the rate of heat production is 600.3 W/m³.

Results

Scale up criterion

A scale up criterion was chosen by examining the incremental ethanol concentrations at various mixing intensities after the reactor contents were distributed from the glass carboy. Figure 3 shows the incremental ethanol concentrations in the four fermenters with different impeller speeds for the two scenarios (35 and 60% starting conversion). It may be seen that the difference in incremental ethanol concentration when $N \geq N_{js}$ is higher than that when $N < N_{js}$ for both scenarios. Statistical analysis on the means for the two groups ($N < N_{js}$ and $N \geq N_{js}$) shows that it is statistically significant to have higher incremental ethanol concentrations operating at the impeller speeds when all particles are suspended ($N \geq N_{js}$) for each scenario. As shown in Fig. 3, there is no clear benefit of increasing impeller speed beyond just-suspension of solids particles for both scenarios. Thus, N_{js} was selected as the operating point for scale up although it seems there is no big difference in incremental ethanol concentrations if operating at lower impeller speeds. The penalty is expected to be higher by operating at partial particle suspension instead of just particle suspension if the reactor contents are not fully mixed for partial particle suspension at the start of the experiments.

Physical parameters

To analyze reactor mixing using industrial mixing analysis and CFD simulation, physical parameters such as liquid density, liquid viscosity, solids density, solids particle size, and solids volume fraction were obtained via experiments. Table 2 shows the measured liquid densities at different cellulose conversions. Liquid density is quite constant during the course of reaction. The average liquid density is 1005.1 g/L which was used for the calculations. Figure 4 shows the measured liquid viscosities and solids densities

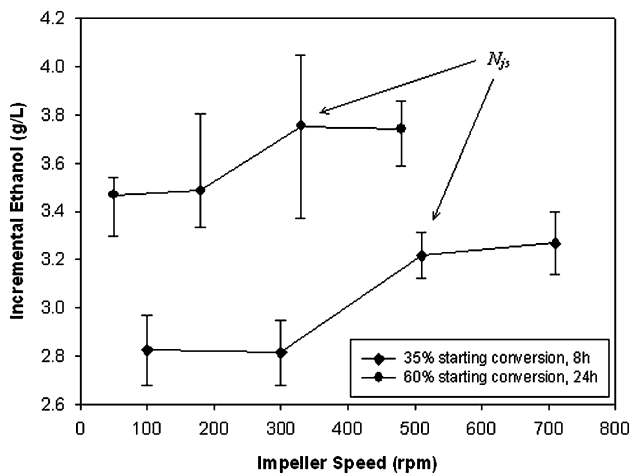


Fig. 3 Reactor performance versus impeller speed (N_{js} was determined visually by observing solids motion at the bottom of the vessel during the experiment using ‘Two Seconds’ criterion, data for 35% starting conversion are the average of duplicate HPLC measurements, data for 60% starting conversion are the average of four HPLC measurements, *error bars* are the lower and higher range of data)

at 37 °C versus cellulose conversions together with linear fit of the data. The fitted equations are

$$\mu_L = 0.2053x + 0.8031 \tag{6}$$

$$\rho_S = 994.0x + 1338.3 \tag{7}$$

with a R^2 value of 0.9986 for liquid viscosities and 0.9937 for solids densities. For the changes in solids densities, more amorphous fibers are hydrolyzed as conversion increases, leaving heavier residues such as calcium carbonate and other paper additives. Table 3 shows the volume weighted average particle diameters at different cellulose conversions. Particle diameters for cellulose conversions within the measured range can be interpolated. For conversion higher than 84%, the particle diameter at 84% conversion can be used for conservative analysis and design. Cellulose conversion in a cascade CSTR configuration with reactor number ≤ 5 is not likely to be lower than 48% in the first reactor if the final conversion is higher than 90%. The volume fraction of total solid particles was calculated based on cellulose and xylan conversions using the following equation

$$VF = \frac{([I]_0 - [C]_0 - [X]_0) + [C]_0(1 - x_C) + [X]_0(1 - x_X)}{\rho_S} \tag{8}$$

where $[I]_0$, $[C]_0$, $[X]_0$, x_C , x_X are initial total solids concentration, initial cellulose concentration, initial xylan concentration, cellulose conversion, and xylan conversion respectively. Yeast was not included in the calculation due to the relatively small volume occupied by cells and the fact that it is readily suspended. Using the above data and correlations, a summary of the values of the physical

Table 2 Liquid density at different conversions

Conversions	Liquid density (g/L)
0.48	1004.5
0.65	1005.8
0.76	1006.1
0.80	1004.2
0.84	1005.1

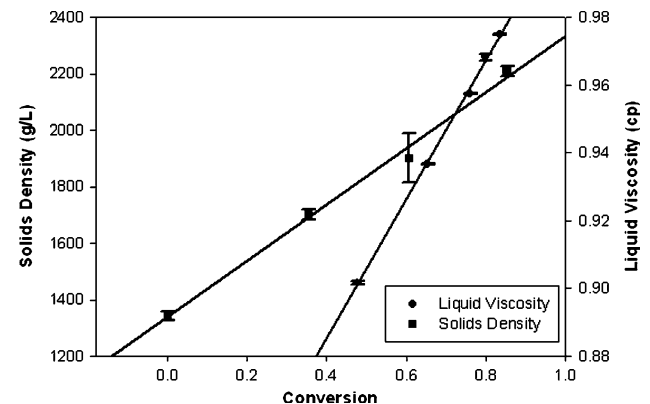


Fig. 4 Liquid viscosity and solids density at different conversions (data are the average of duplicate measurements, *error bars* are the lower and higher range of data)

Table 3 Particle diameters at different conversions

Conversions	Particle diameter (m)
0.48	30.40×10^{-6}
0.65	28.15×10^{-6}
0.76	28.62×10^{-6}
0.80	24.14×10^{-6}
0.84	23.66×10^{-6}

parameters with a cellulose conversion of 48% and a xylan conversion of 35% is presented in Table 4.

N_{js} at lab scale

N_{js} at lab scale was observed right after sampling in the experiments for the measurement of physical properties. The criterion was ‘no particles are stationary on the bottom of the vessel for longer than two seconds’ [21].

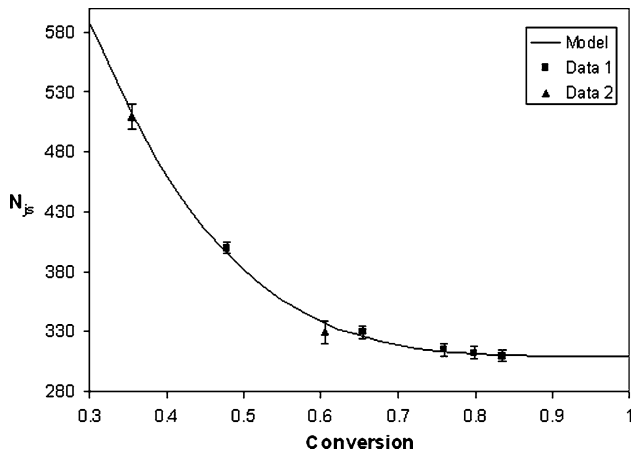
Figure 5 shows the observed N_{js} versus conversion. An equation fit to the data is

$$N_{js} = 1,155(1 - x)^4 + 310 \tag{9}$$

with a root mean square of residual equals to 3.7 rpm. Using Eq. 9, an N_{js} of 395 rpm was calculated for 48% cellulose conversion. The observed solids suspension at N_{js} is quite uniform with cloud height virtually equal to unity. To confirm that CFD is able to predict this observation, two

Table 4 Physical parameter values at 48% cellulose conversion

Physical parameters	Values
Liquid density (Table 2 average)	1005.1 g/L
Liquid viscosity (Eq. 6)	0.9016 cp
Solids density (Eq. 7)	1815.4 g/L
Average particle diameter (Table 3)	30.4×10^{-6} m
Solids volume fraction (Eq. 8)	7.4%

**Fig. 5** Just-suspended Speed (rpm) versus conversion (data points are single observations, error bars are estimated at the time of observation based on varying impeller speed)

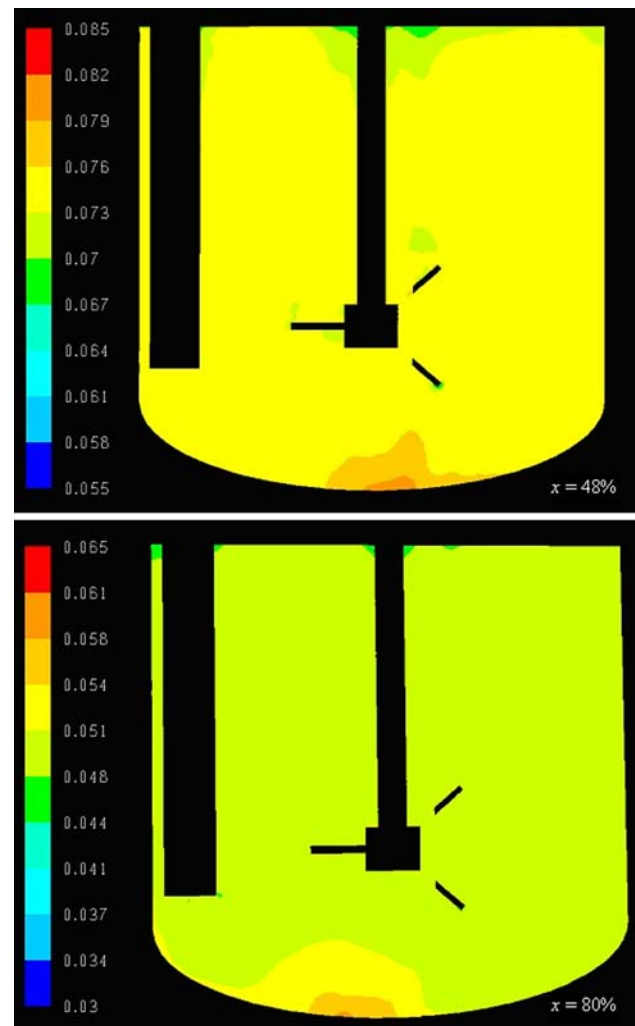
FLUENT simulations were conducted with cellulose conversions at 48 and 80%, respectively. The resulting contours of solids volume fraction in a vertical plane appear in Fig. 6, which shows that CFD is capable of predicting the observations with close to uniform solids suspension for both cases.

Scale up N_{js}

As pointed out in the introduction, two extreme scale-up strategies for N_{js} are constant impeller tip speed and constant power per unit mass. The actual point for N_{js} lies in between these two extreme cases. CFD simulation was used to determine this point. The quality of solids suspension, σ as defined in Eq. 3, is 0.006 for lab scale at 48% cellulose conversion. σ versus impeller speed at large scale is shown in Fig. 7, which implies that an impeller speed of 6 rpm is necessary to achieve the just-suspended condition at large scale. Taking into account gearbox efficiency and conservative analysis, an impeller speed of 7.5 rpm was selected. The power requirement for the impeller calculated according to Eq. 10 is 13.4 kW.

$$P = p_o \rho_{ave} N^3 D^5 \quad (10)$$

The power requirements for scaling up via constant tip speed and constant power per volume are 1.22 and

**Fig. 6** Contour of solids volume fraction at N_{js} with $x = 48\%$ and $x = 80\%$

143 kW, respectively. The power consumption exceeds that required to maintain constant tip speed, but is far less than that for constant power per volume to satisfy N_{js} .

Other mixing requirements

In addition to selection and application of a scale-up criterion and calculation of impeller power requirements, it is useful to check other mixing requirements including liquid phase mixing, solid–liquid mass transfer, and heat transfer.

To check whether liquid phase mixing is adequate, one approach is to compare the characteristic reaction time to the mixing/blend time (the time required for liquid phase to reach 95% of equilibrium concentration). The characteristic reaction time, calculated by Eq. 11, is 4,627 s. The blend times for lab and large scale, calculated by Eq. 12 [22], are 6 and 297 s, respectively.

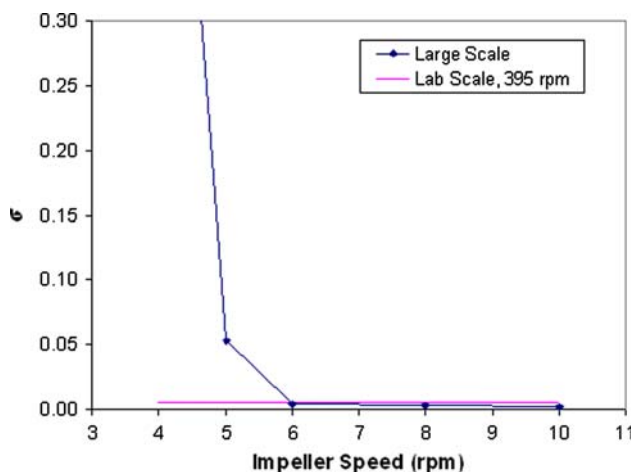


Fig. 7 Solids suspension versus impeller speed for large scale

$$t_r = \frac{1}{k_r} \tag{11}$$

$$N\tau_B = \frac{5.2}{P_o^{1/3}} \left(\frac{T}{D}\right)^2 \quad \text{for } Re > 6,400 \tag{12}$$

The ratio of large scale mixing time to reaction time is larger than 0.01, thus a closer look for liquid phase mixing was to calculate the local Damkoehler number, Da_M , the ratio of reaction rate to local turbulent mixing rate using Eq. 13 in FLUENT. A picture of the Da_M in a vertical plane is shown in Fig. 8. The Damkoehler numbers are all smaller than 0.01, which suggests that liquid phase mixing is fast enough compared to reaction.

$$Da_M = \frac{k_r}{\epsilon} k(x) \tag{13}$$

For particle settling velocity ≤ 0.0005 m/s, which is the case for this study, the correlation for solid–liquid mass transfer reported by Armenante and Kirwan [23] was employed. The correlation is as shown in Eqs. (14) to (17).

$$Sh = 2 + 0.52 Re_p^{0.52} Sc^{1/3} \tag{14}$$

$$Sh = \frac{k_{SL} d_p}{D_A} \tag{15}$$

$$Re_p = \frac{\rho_L \epsilon^{1/3} d_p^{4/3}}{\mu_L} \tag{16}$$

$$Sc = \frac{\mu_L}{\rho_L D_A} \tag{17}$$

Equation 16 suggests that the scale up should be based on constant power per mass/volume, which needs quite excessive power consumption from which the system does not benefit as shown in Fig. 3 as long as the particles are all suspended. To get an idea about scaling up solid–liquid mass transfer at N_{js} , the ratio of mass transfer rate to

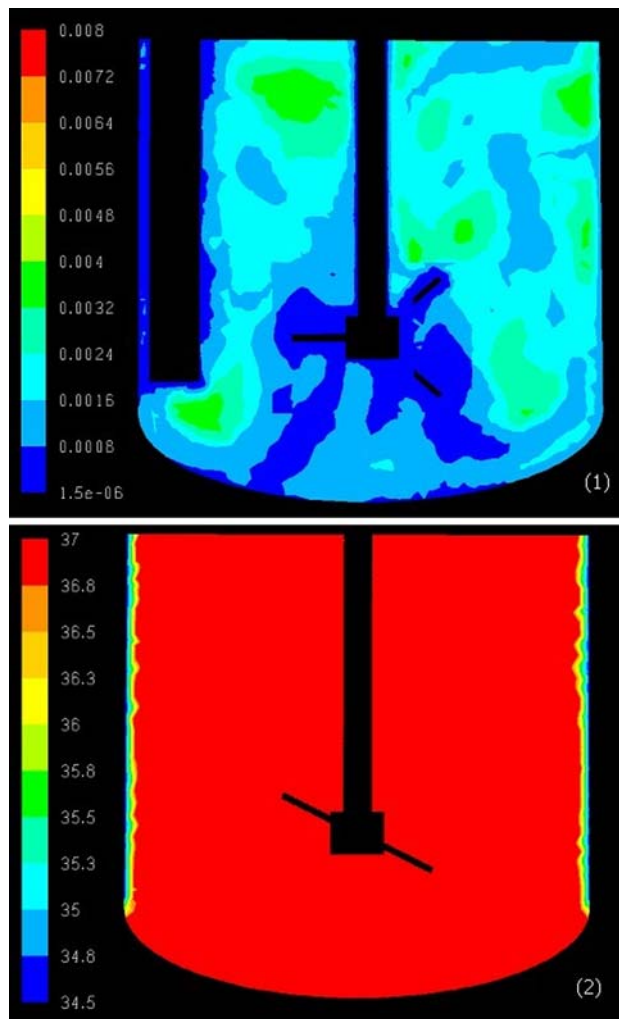


Fig. 8 Local Damkoehler number (1) and temperature profile (2) at large scale

reaction rate was calculated for both lab and large scale using Eq. 18,

$$\frac{M_k}{M_r} = \frac{k_{SL} a_p ([Cb^*] - [Cb])}{k_r [CE]} \tag{18}$$

$$a_p = 6 \frac{\phi}{\rho_S d_p} \tag{19}$$

where [CE], [Cb], [Cb*], and ϕ are cellulose–enzyme complex concentration, bulk cellobiose concentration, interphase cellobiose concentration (cellobiose solubility in water), and solids loading with a unit of kilogram solids per cubic meter solid-free liquid. The calculation used water molecular diffusivity for D_A . The ratio at lab scale is 29.5, while the ratio at large scale is 23.5 with conservative calculation using the highest reaction rate. This suggests that mass transfer at just-suspended speed is adequate at large scale.

Heat transfer to remove the heat of reaction is a design issue for ethanol fermentation. There are different approaches for heat transfer including vessel with a jacket, use of an internal surface (heat exchanger), reflux cooling by solvent evaporation, and pump around loop with external heat transfer. In this study, vessel wall jacket was analyzed both using correlations and FLUENT simulation. The correlation uses Eqs. (20) to (23).

$$\frac{h_i T}{k_L} = 0.45 Re^{2/3} Pr^{1/3} \quad (20)$$

$$Pr = \frac{\mu_L C p_L}{k_L} \quad (21)$$

$$Re = \frac{\rho_L N D^2}{\mu_L} \quad (22)$$

$$h_i \Delta T = Q \quad (23)$$

Because there is no correlation for the marine impeller used in this study, the exponents in Eq. 20 were taken for a pitched blade turbine with four blades [24], which has a similar power number to the marine impeller. Water thermal conductivity and heat capacity were used. The calculated temperature drop is 2.6 °C for the system, which is about the same (2.5 °C) as shown in Fig. 8 simulated in FLUENT. This low level of heat transfer requirement is due to slow reaction and low level of heat of production in anaerobic fermentation as compared to aerobic fermentation, 54 Kcal/mol compared to 686 Kcal/mol of glucose consumed.

Discussion

The absence of systematic scale up approach for biological conversion of cellulosic biomass to commodity product presents a challenge for successful commercialization. A reliable scale up strategy is desirable to reduce risk, inform process decisions, and reduce cost from pilot and demonstration operations.

In this work, a scale up procedure was developed for SSF reactors using waste paper sludge as the feedstock. Through bench scale experiments, just-suspension of solid particles was identified as the desired point of operation with regard to mixing intensity and was selected as the scale up criterion. There is no clear benefit of increasing impeller speed beyond N_{js} in terms of enhanced reactor performance. This suggests that reaction is the rate limiting step at N_{js} , since reactor performance should increase due to increasing agitation if mass transfer were rate limiting as can be seen from Eqs. (14) to (17). Reaction is still the rate limiting step at the large scale analyzed in this study because the rate of mass transfer is still more than ten times

higher than that of reaction based on conservative calculations.

The scale up exponent for N_{js} is dependent on the properties of liquid and particles in the system [16, 25, 26]. Once the solid particles are suspended, the amount of power input required from agitation is to provide the energy to overcome particle settling and fluid deflection and friction at the internal tank surface. Thus, two extreme cases for scaling up the power required for N_{js} will be in a form of either $P \sim V$ (constant power per volume) or $P \sim S$ (constant tip speed). The power from agitation for the same geometry during scale up can also be expressed as

$$P \sim N_{js}^3 T^5 \quad (24)$$

which, by substituting, will give the following correlations

$$P \sim V \Rightarrow N_{js} \sim T^{-2/3} \quad (25)$$

$$P \sim S \Rightarrow N_{js} \sim T^{-1} \quad (26)$$

For particles that have a slow settling velocity, the amount of energy required to overcome the settling of the particles is small. Thus, the scale up exponent will be close to -1. However, scale up of such system using an exponent of -1 will be under estimate required power whereas using an exponent of $-2/3$ over estimate power. Using CFD, an exponent of -0.88 was calculated for suspension of the feedstock investigated in this study.

The predicted low level of mixing requirement is due to a combination of small particle size, low solids density, and low liquid viscosity, which can be observed in Eq. 27 derived from the Zwietering equation [12].

$$P_{js} \sim \left(\frac{\rho_s - \rho_L}{\rho_L} \right)^{1.35} d_p^{0.6} \mu_L^{0.3} \quad (27)$$

Mixing requirements would be much higher were the solids unreacted as opposed to being in a steady-state CSTR. Thus it is important to avoid high concentrations of unreacted during start-up. The predicted power requirement (13.4 kW) is comparable to industrial implementation in a corn dry mill with the same scale using a batch reactor configuration (18.6 kW). For corn ethanol production, the power is likely not enough for good mixing for a period of time after the start of a batch due to higher viscosity and large particle size, but the mixing improves when particle size and liquid viscosity are reduced as reaction proceeds. Operation of a paper sludge SSF reactor in a similar batch mode could be considered. The practicality of this would be determined primarily by the starting conditions of the system. If there is little or no free flow liquid, the impeller would likely not be able to move, making batch operation infeasible.

To analyze the second and following reactors, kinetic model will be used to predict cellulose conversion. The model assumes ideal residence time distribution as a result of perfect mixing. This is true as long as there is no channeling between inlet and outlet because the ratio of residence time to mixing time is at least 280 even at the large scale.

Acknowledgments The authors are grateful for the support provided by funding from grant No. 60NANB1D0064 from the National Institute of Standards and Technology.

References

- Lynd LR, Wyman CE, Gerngross TU (1999) Biocommodity engineering. *Biotechnol Prog* 15(5):777–793
- Wyman CE (2003) Potential synergies and challenges in refining cellulosic biomass to fuels, chemicals, and power. *Biotechnol Prog* 19(2):254–262
- DOE (2007) http://www1.eere.energy.gov/biomass/printable_versions/economic_growth.html. Accessed Sept 2008
- McLaughlin SB, Ugarte D, Garten CT et al (2002) High-value renewable energy from prairie grasses. *Environ Sci Technol* 36(10):2122–2129
- Tyson KS (1993) Fuel cycle evaluations of biomass–ethanol and reformulated gasoline, vol I. NREL/TP-463-4950, DE94000227
- Wang M, Saricks C, Santini D (1999) Effects of fuel ethanol use on fuel-cycle energy and greenhouse gas emissions. Center for Transportation Research, Argonne National Laboratory. ANL/ESD-38
- Delucchi M (1991) Emissions of greenhouse gases from the use of transportation fuels and electricity. ANL/ESD/TM-22. Center for Transportation Research. Argonne National Lab. Publication No. UCD-ITS-RP-91-30
- Wyman CE (1994) Alternative fuels from biomass and their impact on carbon dioxide accumulation. *Appl Biochem Biotechnol* 45(46):897–915
- Atiemo-Obeng VA, Penney WR, Armenante P (2004) Solid–liquid mixing. In: *Handbook of industrial mixing: science and practice*. Wiley, NY
- Elander R (1988) M.S. thesis: Mixing Requirements for Enzymatic Hydrolysis of Cellulose. Department of Agricultural and Chemical Engineering, Colorado State University. Fort Collins, Colorado
- Huang AA (1975) Kinetic Studies on Insoluble Cellulose–cellulase system. *Biotechnol Bioeng* 17(10):1421–1433
- Zwietering TN (1958) Suspending of solid particles in liquid by agitators. *Chem Eng Sci* 8:244–253
- Baldi G, Conti R, Alaria E (1978) Complete suspension of particles in mechanically agitated vessels. *Chem Eng Sci* 33:21–25
- Raghav Rao KSMS, Rewatkar VB, Joshi JB (1988) Critical impeller speed for solid suspension in mechanically agitated contactors. *AIChE J* 34(8):1332–1340
- Corpstein RR, Fasano JB, Myers K (1994) The high-efficiency road to liquid–solid agitation. *Chem Eng* 101:138–144
- Geisler RK, Buurman C, Mersmann AB (1993) Scale-up of the necessary power input in stirred vessels with suspension. *Chem Eng J* 51:29–39
- Shao X, Lynd L, Wyman C (2009) Kinetic modeling of cellulosic biomass to ethanol via simultaneous saccharification and fermentation: Part II. Experimental validation using waste paper sludge and anticipation of CFD analysis. *Biotechnol Bioeng* 102(1):66–72
- Ghose TK (1987) Measurement of cellulase activities. *Pure Appl Chem* 59(2):257–268
- Kadam KL, Newman MM (1997) Development of a low-cost fermentation medium for ethanol production from biomass. *Appl Microbiol Biotechnol* 47:625–629
- Shao X, Lynd L, Wyman C et al (2009) Kinetic modeling of cellulosic biomass to ethanol via simultaneous saccharification and fermentation: Part I. Accommodation of intermittent feeding and analysis of staged reactors. *Biotechnol Bioeng* 102(1):59–65
- Brown DAR, Jones PN, Middleton JC et al (2004) Experimental methods. In: *Handbook of industrial mixing*. Wiley, NY
- Grenville RK (1992) Ph.D. thesis: Blending of viscous Newtonian and pseudo-plastic fluids. Cranfield Institute of Technology. Cranfield, Bedfordshire, England
- Armenante PM, Kirwan DJ (1989) Mass-transfer to microparticles in agitated systems. *Chem Eng Sci* 44(12):2781–2796
- Penney WR, Atiemo-Obeng VA (2004) Heat transfer. In: *Handbook of industrial mixing: science and practice*. Wiley, NY
- Molerus O, Latzel W (1987) Suspension of solid particles in agitated vessels – I. Archimedes number ≤ 40 . *Chem Eng Sci* 42(6):1423–1430
- Molerus O, Latzel W (1987) Suspension of solid particles in agitated vessels – II. Archimedes number > 40 , reliable prediction of minimum stirrer angular velocities. *Chem Eng Sci* 42(6):1431–1437